ISSN 1831-9424

JRC TECHNICAL REPORT

DWAM – Dynamic Properties of Electron Beam Welded Specimens

Open Access to JRC Research Infrastructures
Call 2019-1-RD-ELSA-Hoplab: User Access Report
HopLab, Hopkinson Bar facility

Peroni, M; Tsionis, G, Croteau, JF, Cantergiani, E; Atieh, S

2022

Joint Research Centre

EUR 31230 EN

Contact information
Name: Marco Peroni
Address: Via E. Fermi, 2749, 21027 Ispra (VA), Italy
Email: marco.peroni@ec.europa.eu
Tel.: 00390332789775

EU Science Hub
https://joint-research-centre.ec.europa.eu

JRC129472

EUR 31230 EN

PDF ISBN 978-92-76-57036-3 ISSN 1831-9424 doi:10.2760/506325 KJ-NA-31-230-EN-N

Luxembourg: Publications Office of the European Union, 2022

How to cite this report: Peroni, M; Tsionis, Croteau, J F, Cantergiani, E, Atieh, S, *DWAM - Dynamic Properties of Electron Beam Welded Specimens; Call 2019-1-RD-ELSA-HopLab: User Access Report*, Publications Office of the European Union, Luxembourg, 2022, doi:10.2760/506325, JRC129472.

Contents

Abstract

This report presents the technical aspects of the experimental test campaign relevant to the project "DWAM - Dynamic Properties of Electron Beam Welded and Additively Manufactured Specimens", whose proposal was successfully reviewed and selected in the framework of the JRC OPEN ACCESS programme. The research conducted concerns the investigation of the tensile and compressive mechanical behaviour at high strain-rates of two materials (OFE copper and niobium) subjected to electron beam welding. Specimens were provided by the User. It was agreed between JRC and the User Access Team not to test the additively manufactured specimens that were foreseen in the proposal and test instead a bigger number of electron beam welded specimens.

According to the project proposal, samples preparation was done by the User Access Team and the testing programme was elaborated and jointly agreed with the ELSA-HopLab laboratory staff. Preliminary static tests were performed by the User Access Team at ENSTA Bretagne in order to provide the HopLab technicians with initial data for setting up the dynamic testing campaign.

The subsequent tests execution has been done completely by the ELSA-HopLab laboratory staff. Static and low strain-rate tests have been performed on an MTS standard testing machine. High strain-rate tests have been carried out using two Hopkinson bar facilities for ductile materials (Laboratory E06).

Due to the pandemic crisis (COVID), the preliminary scientific program has been slightly modified (no additive manufactured specimens have been tested) and the User Access Team was not present during the tests because of the safety rules in force at the JRC Ispra site. To mitigate the effect of these limitations, all the tests results have been discussed during daily meetings between the User Access Team and ELSA staff.

The report also presents the elaboration of the raw experimental data in order to obtain the forces and displacements directly applied to the specimens during the tests. The scope of this section is not to draw considerations about the behaviour of the tested specimens but rather to present an overview of the experimental data obtained with the test campaign. Finally, a description of the storage structure of the elaborated data has been included, which will help future users to effectively manage and use the data for their purposes.

The project has reached its objectives and the activity is deemed a success by both parties. The obtained experimental data are of high quality and of significant scientific interest for the advanced manufacturing processes and materials investigated.

Foreword

The European Commission's Joint Research Centre (JRC) opens its scientific laboratories and facilities to people working in academia and research organisations, industry, small and medium enterprises (SMEs), and more in general to the public and private sector.

Offering access to visiting researchers is part of JRC's strategy to:

- enhance dissemination of scientific knowledge;
- boost competiveness;
- bridge the gap between research and industry;
- provide training and capacity building.
- Scientists have the opportunity to work in the following fields:
- nuclear safety and security (Euratom Laboratories);
- chemistry;
- biosciences/life sciences;
- physical sciences;
- ICT;
- Foresight.

The present document constitutes the "User Access Report", which summarises the results from the access given to the Hopkinson Bar facility (HopLab).

Authors

JRC Research Infrastructure (HopLab, Hopkinson Bar)

- Peroni, M
- Tsionis, G

User Access Project (DWAM - Dynamic Properties of Electron Beam Welded and Additively Manufactured Specimens)

- Croteau, J F (Lead User, ENSTA Bretagne)
- Cantergiani, E (I-Cube Research – Bmax)
- Atieh, S (CERN)

1 Introduction

I-Cube Research - Bmax develop fast forming technologies (i.e. electro-hydraulic forming and magnetic pulse forming) for different metals and applications (automotive, particle accelerators, luxury packaging, etc...) and the ENSTA Bretagne is a leading European university in material characterisation and modelling at high strain rates. In the frame of a collaboration with the European Organization for Nuclear Research (CERN) for the fast forming of superconducting radio frequency cavities, I-Cube Research - Bmax need to study the behaviour of welds under high strain-rate loading. To perform predictive simulations of the electro-hydraulic forming process, the evolution of material behaviour as function of strain-rate is crucial. The main scope of this activity is to study, for the first time, the behaviour of electron beam welds (EBW) of copper and niobium at high strain-rates and to extract a constitutive model from experimental results to be implemented in simulations of the electro-hydraulic forming process. It is of great interest in the production of particle accelerators to avoid rupture of pre-welded components during forming at high strain-rates. A series of preliminary tests on not welded specimens have been carried out by the User Access Team and the data have been used as starting point to design the test campaign.

Tests have been performed at ELSA HopLab both in tension and in compression using different rigs according to the testing conditions and velocity, as will be described in the next section. Whereas the testing campaign could appear as a conventional industrial application without substantial difficulties and scientific interest, this experimentation presented several challenges due to the mechanical properties of the tested materials. Niobium and copper are in fact very ductile materials with low yield stress and this feature makes problematic the specimen manufacturing and manipulation with conventional machining procedures. In addition, conventional grips or fixture systems adopted in testing machines are not suitable for these materials because they can damage the specimens before starting the tests. To overcome this problem, a new specimen geometry has been developed by ELSA staff applying the electrical discharge machining technique. As a result, specimens with the proposed geometry are simpler to manufacture (and substantially cheaper) and can fit different testing machines arranged with proper grips/fixtures for soft materials.

Moreover, the adoption of optical measurement techniques substantially increased the amount of data available. On the other hand, the complexity of the tests increased (e.g. because of problems with adhesion of the paint on the particular materials surfaces).

Concerning the logistics of the project, the activity took place in July 2020 during the COVID pandemic emergency and observing all the safety rules in force at the JRC Ispra site. The experimental tests were carried out exclusively by the ELSA-HopLab staff under the scientific supervision of Marco Peroni. The User team has been informed about the test progress with daily online meetings and documenting the tests with a series of photo-sequences. In practice, ELSA staff performed preliminary tests and elaborated the data for each adopted setup, and then deeply discussed the results with the User team before completing the tests.

2 Specimen manufacturing

As mentioned before, the specimens have been provided by the user and have been manufactured by CERN with two different materials: oxygen-free electronic (OFE) copper (ASTM C10100 [1]) and high-purity niobium (residual-resistivity ratio > 300). Sheets with an initial thickness of 4 mm were electron beam (EB) welded with one pass on each side of the sheet using the same electron beam parameters (accelerating voltage: 100 kV, current: 22-23 mA, work piece distance: 400 mm, and beam speed: 600 mm/min). The top and bottom surfaces of the welded sheets were milled to remove surface defects produced during welding and obtain flat surfaces. Specimens were cut using wire electro-discharge machining as shown in Figure 1 (left). In addition, OFE copper specimens were annealed at 600°C for 2 hours in vacuum after EB welding.

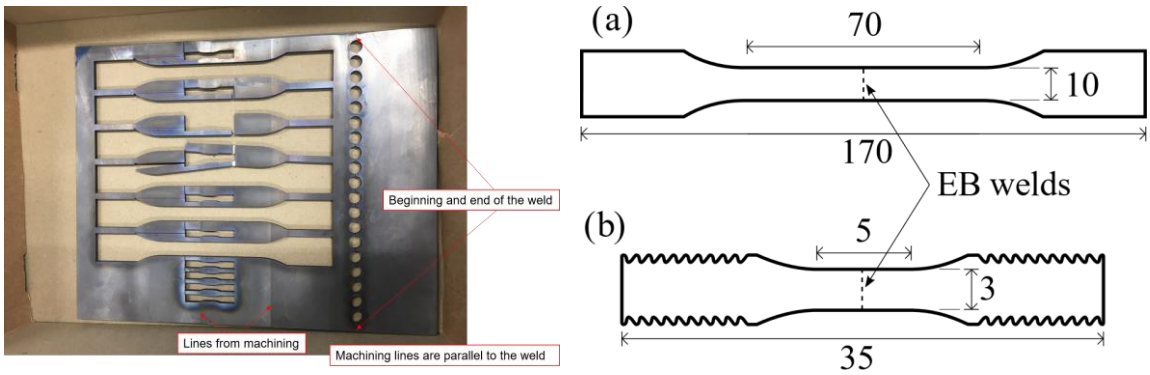

Figure 1. Electron beam welded niobium sheet after the specimens were cut (left) and adopted geometries and dimensions (in mm) of the specimens for the tensile tests (right).

For the specimens tested in tension, the weld was located at the centre of the gage section and perpendicular to the direction of the tensile action, as specified in the ISO 4136:2012 standard [2]. Two geometries have been adopted as reported in Figure 1 (right). The upper one is a 'standard' geometry for tensile tests adopted to investigate the material behaviour at three different strain-rates (0.001, 0.01 and 0.1 1/s). However, this geometry is not suitable to perform high strain-rate tests (it is too large to be connected to the equipment bars that typically have a diameter of 10 mm) and for this reason, a different one has been developed (Figure 1 right-bottom). This geometry, for the smaller size, is compatible with high strain-rate tests by means of Hopkinson bar facilities, is easier to manufacture compared to the geometry with threaded ends and compatible with materials only available in sheets. The smaller specimens have been tested in tension at five strain-rate levels (0.002, 0.2, 20, ~400 and ~1500 1/s).

Analogously, the specimens tested in compression have been obtained with the same methodology (see Figure 1 left) and present a cylindrical shape with diameter D = 8 mm and height H = 4 mm. The EBW welding is perpendicular to the specimen axis and the test represents a typical material solicitation during electro-hydraulic forming and magnetic pulse forming to produce half-cells for SRF cavities, when the sheet is compressed through its thickness upon impact with a rigid die. Indeed, the weld would undergo mainly equibiaxial tensile stresses during "free" expansion of the sheet, but it would experience compressive stresses at high strain rate during impact of the sheet with the die. Moreover, electron beam welding is known to limit the heat affected zone compared to standard welding techniques, but the heat affected zone can still be marked on niobium, which showed larger grain size at the weld zone and then a decreasing grain size moving far from the weld. The authors were interested to test this discontinuity in grain sizes both in tension and compression at high strain rates. The specimens have been tested in compression at four strain-rate levels (0.001, 0.1, 10 and ~3000 1/s respectively).

Since specimens have been manufactured under the responsibility of the User team, ELSA staff took care of the specimen preparation for what concerns digital image correlation (DIC) measurements. In this context, a speckle pattern has been created on the surface of each specimen to efficiently adopt DIC algorithms and accurately elaborate each test photo-sequence. All specimens tested under static and low velocity loads have been painted with a white acrylic primer and subsequently a black speckle has been applied with a black acrylic paint.

Adhesion problems have been observed with increasing test velocity, due the material tested (acrylic paints are normally used in the automotive sector on steel and aluminium), in particular on OFE copper specimens (experiments b05 and b06). In practice, the paint layer flaked off at the beginning of the tests, making

difficult to apply DIC algorithms (acceptable data were anyway obtained). Figure 2 presents an example of this phenomenon: the white over-exposed zones are the points where paint flaked off exposing the high-reflective underlying metal. For this reason, the specimens for the high-speed tests have been treated differently to increase the paint adhesion by grinding the specimen surface and accurately cleaning it with a solvent. In addition, only one paint layer with the stochastic pattern has been adopted (white for niobium and black for OFE copper) to avoid the creation of a brittle layer on the surface of the specimen.

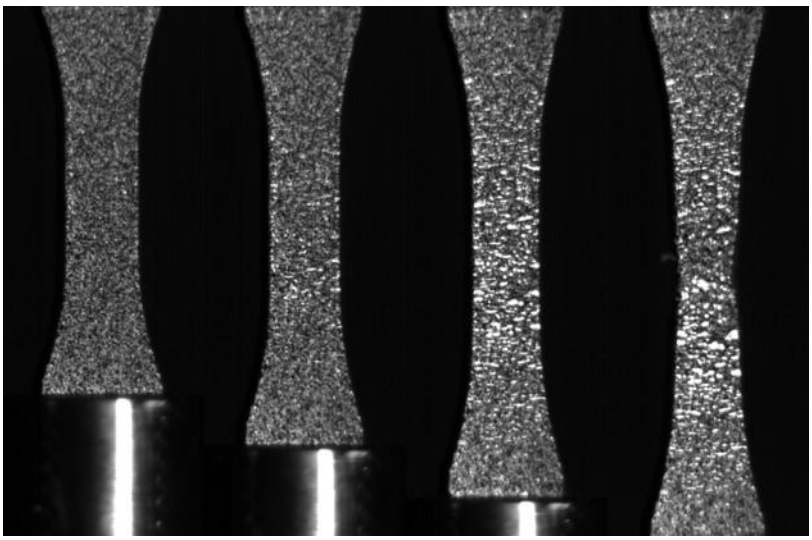

Figure 2. Paint flakes off on copper specimen at 100 mm/s test (b05)

With this treatment modification, no further problems of paint flake off have been observed also at substantially higher velocities.

3 Test equipment and execution

As requested by the User team, both materials have been tested at different velocities of deformation in order to assess the effect of the strain-rate on the material behaviour. Due to the large range of strain-rates investigated, the tests have been performed with two different experimental apparatuses.

Static tests and low strain-rate tests (up to 200 mm/s of actuation speed) have been performed on a MTS universal testing machine and adopting a DIC measuring system.

High strain-rate tests have been performed using the Hopkinson Bar technique and in particular using two bars that were designed ad-hoc for metals. DIC was also used for these tests.

In the next sections a short description of the equipment is given, including the detailed list of instruments and sensors employed.

3.1 MTS Servo-hydraulic testing machine (static and low strain-rate tests)

As mentioned before, the static and low strain-rate tests have been performed with an MTS universal testing machine (810 Material Testing System with maximum force of 50 kN) controlled with the FlexTest 40 Digital controller unit. For both static and low strain-rate tests, a camera was used to acquire a sequence of photos synchronized with the tensile machines' data acquisition sensors (i.e. the force derived by the load cell and the piston displacement recorded with a linear variable differential transformer LVDT).

3.1.1 Tensile tests ('standard' geometry)

For the tensile tests performed on the 'standard' geometry specimens, forces and displacements have been directly recorded by the FlexTest 40 unit and synchronized with a high-resolution camera (PCO edge 5.5). Illumination was provided by two cold lights (Veritas Constellation 120) as presented in Figure 3.

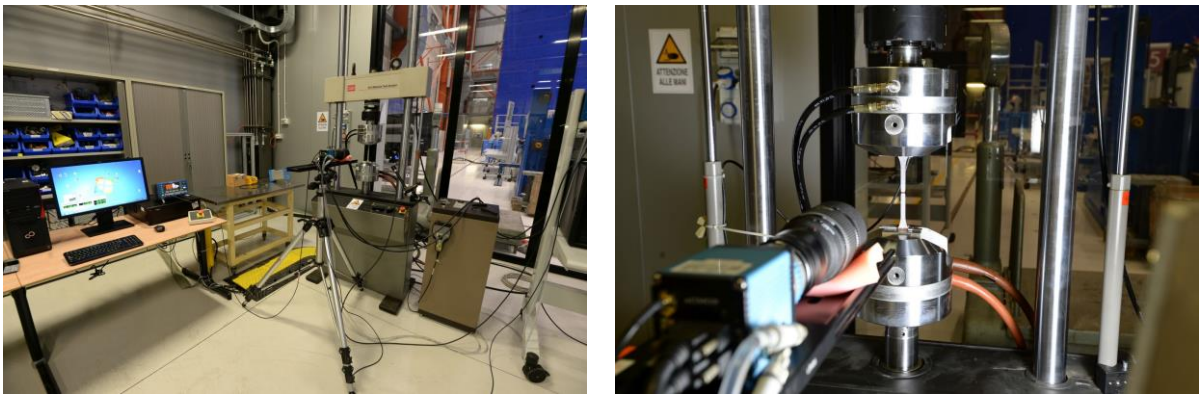

Figure 3. Testing setup for tensile tests on 'standard' geometry specimens (left) and closer view of the specimen and loading equipment (right)

To clamp the specimen a couple of hydraulic grips was used. A reduced actuating pressure has been imposed to limit the deformation of the specimen ends due to the low strength of the tested materials.

Table 1 summarizes the tensile tests performed on the specimens with 'standard' geometry and at the three different strain-rate levels, as required by the User team. In Table 1, as in the following tables, the authors chose to report the average test velocity instead of the specimen strain-rate. This was due to the fact that the latter is not constant during the test and depends on the specimen strain field. The strain-rate could be precisely evaluated by the users using DIC methodology or simulating every test with the same experimental constrains.

Table 1. Tensile tests ('standard' geometry).

Test Label	Test Type	Velocity (mm/s)	Date	Material
c01	Monotonic MTS	0.08	30/06/2020	OFE Copper
c02	Monotonic MTS	0.08	30/06/2020	OFE Copper
c03	Monotonic MTS	0.8	30/06/2020	OFE Copper
c04	Monotonic MTS	0.8	30/06/2020	OFE Copper

c05	Monotonic MTS	8	30/06/2020	OFE Copper
c06	Monotonic MTS	8	30/06/2020	OFE Copper
f01	Monotonic MTS	0.08	30/06/2020	Niobium
f02	Monotonic MTS	0.08	30/06/2020	Niobium
f03	Monotonic MTS	0.8	30/06/2020	Niobium
f04	Monotonic MTS	0.8	30/06/2020	Niobium
f05	Monotonic MTS	8	30/06/2020	Niobium
f06	Monotonic MTS	8	30/06/2020	Niobium

3.1.2 Tensile tests ('high strain-rate' geometry)

For the tensile tests on the 'high strain-rate' geometry specimens two setups were adopted: one for static tests (strain-rate about 0.002 1/s) and one for strain-rates up to 20 1/s. The setup for the static tests was similar to the one adopted for the tests on the specimens with 'standard' geometry. In detail, forces and displacements have been directly recorded by the FlexTest 40 unit and synchronized with a camera (PCO edge 5.5), and illumination was provided by two cold lights (Veritas Constellation 120). The only difference was in the fixtures: the hydraulic grips have been replaced by a custom solution as presented in Figure 4. The two grip ends (slightly dark components in Figure 4 right) have been machined to reproduce the opposite profile of the specimen ends with a reduced mechanical play. The specimen mounting is quite simple: it is inserted in the proper slot transversally to the tensile direction.

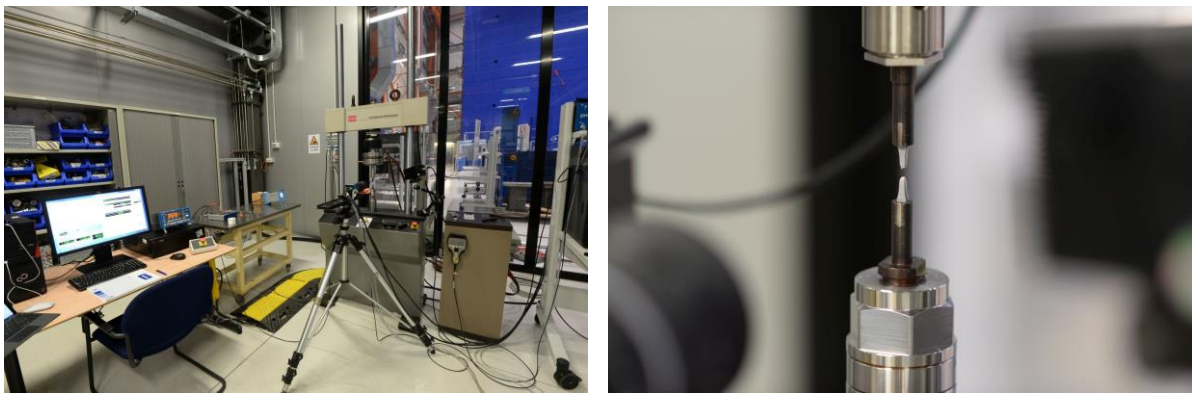

Figure 4. Testing setup for tensile tests on specimens with the 'high strain-rate' geometry (left) and closer view of the specimen and loading equipment (right)

Tests at higher velocity (up to 100 mm/s) have been performed with the same mechanical testing rig but adopting a faster data acquisition system and camera. Specifically, the MTS displacement and force signals have been recorded with a National Instruments acquisition board (NI USB-6366) controlled with the Labview software. To ensure greater measurement performance at these velocities, an additional piezo-electric load cell (Kistler 9361B) has been installed and connected to a charge amplifier (Kistler 5015). Due to the greater resonance frequency of the piezoelectric load cells, the force measurements acquired with this device are not influenced by the applied load (in this range of velocity), thus ensuring the absence of ringing phenomena (resonance of the measuring load cell). Finally, a faster camera has been used to record a suitable number of frames during the test. This was an IDT OS8-S3 high-speed camera synchronized with the National Instruments acquisition board and the Veritas lights.

Table 2 summarizes the tensile tests performed on the specimens with 'high strain-rate' geometry at static and intermediate strain-rates as required by the User team.

Table 2. Static and intermediate velocity tensile tests ('high strain-rate' geometry).

Test Label	Test Type	Velocity (mm/s)	Date	Material
b01	Monotonic MTS	0.01	03/07/2020	OFE Copper
b02	Monotonic MTS	0.01	03/07/2020	OFE Copper
b03	Monotonic MTS	1	03/07/2020	OFE Copper
b04	Monotonic MTS	1	03/07/2020	OFE Copper
b05	Monotonic MTS	100	03/07/2020	OFE Copper
b06	Monotonic MTS	100	03/07/2020	OFE Copper

e01	Monotonic MTS	0.01	03/07/2020	Niobium
e02	Monotonic MTS	0.01	03/07/2020	Niobium
e03	Monotonic MTS	1	03/07/2020	Niobium
e04	Monotonic MTS	1	03/07/2020	Niobium
e05	Monotonic MTS	100	03/07/2020	Niobium
e06	Monotonic MTS	100	03/07/2020	Niobium

3.1.3 Compression tests

Compression tests have been performed with the two setups adopted for the tensile tests on the smaller specimens with 'high strain-rate' geometry. The only difference is related to the final metal inserts of the testing machine that are suitable to perform tests on small metallic cylinder specimens as shown in Figure 5.

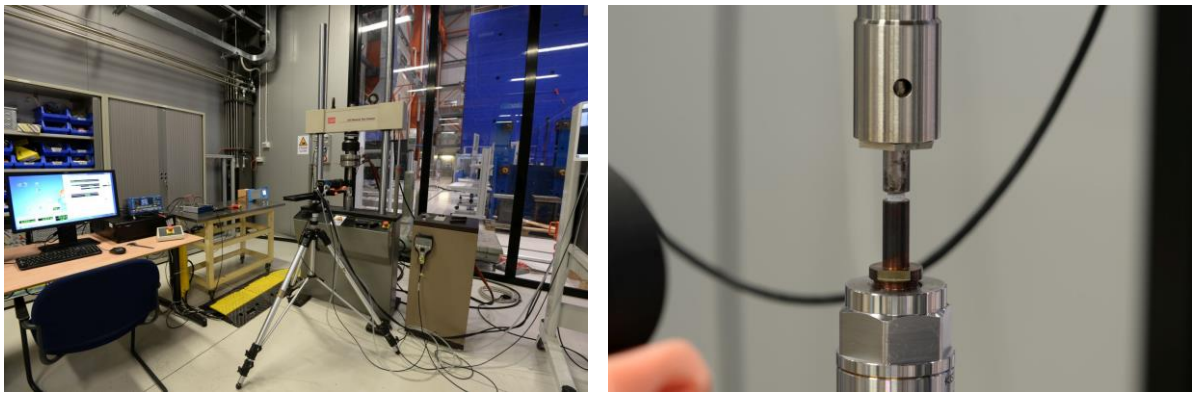

Figure 5. Testing setup for compression tests (left) and closer view of the specimen and loading equipment (right)

In these tests, the welding location is not fixed in the middle of the specimen gage length as in the tensile test. For this reason, all specimens have been oriented maintaining the EBW welding axis parallel to the camera axis. With this procedure, the central portion of the specimen of each test sequence corresponds to the welding zone.

Table 3 summarizes the compression tests performed at static and intermediate strain-rate as required by the User team. In this case and due to the higher number of available specimens, three repetitions have been performed for each velocity, instead of the two carried out for tensile tests.

Table 3. Static and intermediate velocity compression tests.

Test Label	Test Type	Velocity (mm/s)	Date	Material
a01	Monotonic MTS	0.004	08/07/2020	OFE Copper
a02	Monotonic MTS	0.004	08/07/2020	OFE Copper
a03	Monotonic MTS	0.004	08/07/2020	OFE Copper
a04	Monotonic MTS	0.4	08/07/2020	OFE Copper
a05	Monotonic MTS	0.4	08/07/2020	OFE Copper
a06	Monotonic MTS	0.4	08/07/2020	OFE Copper
a07	Monotonic MTS	40	08/07/2020	OFE Copper
a08	Monotonic MTS	40	08/07/2020	OFE Copper
a09	Monotonic MTS	40	08/07/2020	OFE Copper
d01	Monotonic MTS	0.004	08/07/2020	Niobium
d02	Monotonic MTS	0.004	08/07/2020	Niobium
d03	Monotonic MTS	0.004	08/07/2020	Niobium
d04	Monotonic MTS	0.4	08/07/2020	Niobium
d05	Monotonic MTS	0.4	08/07/2020	Niobium
d06	Monotonic MTS	0.4	08/07/2020	Niobium
d07	Monotonic MTS	40	08/07/2020	Niobium
d07	Monotonic MTS	40	08/07/2020	Niobium
d08	Monotonic MTS	40	08/07/2020	Niobium

Before starting the testing phase, the stiffness of the machine has been identified with a void test (a test without the specimen). Using this parameter, in fact, it is possible to improve the evaluation of the Young modulus of the tested material without a proper extensometer applied on the specimen.

3.2 Hopkinson Pressure Bar (high strain-rate tests)

As mentioned above, high strain-rate compression and tensile tests have been performed on two particular Hopkinson bar setups that were specifically designed for metals and in general ductile materials. Both setups have been equipped with the same instrumentation and they have been designed with the same philosophy. The mechanical frame was assembled using aluminium Bosch-Rexroth profiles (save the steel base essential to pre-stress a portion of the input bar in the tensile setup) with ad-hoc supports for the bars equipped with Teflon bushings to reduce friction. The bars present a diameter of 10 mm and are made of high-strength stainless steel 17-4PH. Both input and output bars are equipped with strain-gages (Tokyo Measuring Instruments Laboratory FLA-2-350-11) in a half-bridge configuration. The Wheatstone bridge signal is amplified using a strain-gage amplifier with a cut-off frequency of 500 kHz (EFS SGA02 high-speed) and then recorded at a sample-rate of 10 MHz with a fast transient recorder (GAGE CSE8482-H2).

In addition to the classical Hopkinson bar instrumentation, a high-speed camera (Photron SA1.1) has been used to capture a sequence of photos for each test (frame-rate of 50000 frames per second) and was synchronized with the transient recorder. The same cold lights Veritas Constellation 120, adopted in the static and low strain-rate tests, have been used to ensure the optimal illumination during the tests.

3.2.1 Tensile tests ('high strain-rate' geometry)

The machine adopted for the tensile tests is an example of the so-called "modified Hopkinson bar" because the input pulse is generated through the pre-stressing of a portion of the input bar and quickly released, and not by the impact of the striker bar accelerated with a gas gun apparatus. This design has the great advantage that very long waves can be generated (up to 3 ms of duration in this setup, compared with a typical value of 0.2 ms obtainable with a gas gun) guarantying a large displacement applied to the specimen. In addition, the generated long pulse allows slowing down the test velocity, thus extending the operating range of the equipment.

The total length of the equipment is about 16 m and was obtained by assembling (with properly designed joints) 3 m long bars, as shown in Figure 6. The particular fixtures, essential to fit the particular specimen geometry adopted, have been welded to the bar using EBW technology thanks to the support of the User team and CERN (Figure 6 right). With this manufacturing process, the fixtures do not present any discontinuity with the equipment bars, thus improving the results quality (no spurious reflections are generated by acoustic impedance discontinuities).

Figure 6. Testing setup for Split Hopkinson Pressure Bar (SHPB) tensile tests (left) and closer view of the specimen and loading equipment (right)

Table 4 summarizes the tensile tests performed at two strain-rate levels as required by the User team. Test b10 on the last copper specimen is reported in red in the table because the test failed. In agreement with the User team, the setup has been pushed to the limit to increase the strain-rate - obviously reducing the reliability of the testing system.

Table 4. High-velocity tensile tests (specimens with 'high strain-rate' geometry).

Test Label	Test Type	Velocity (mm/s)	Date	Material
b07	Monotonic SHPB	2500	21/07/2020	OFE Copper

b08	Monotonic SHPB	2500	21/07/2020	OFE Copper
b09	Monotonic SHPB	8000	21/07/2020	OFE Copper
b10	Monotonic SHPB	-	21/07/2020	OFE Copper
e07	Monotonic SHPB	2500	21/07/2020	Niobium
e08	Monotonic SHPB	2500	21/07/2020	Niobium
e09	Monotonic SHPB	8000	21/07/2020	Niobium
e10	Monotonic SHPB	8000	21/07/2020	Niobium

3.2.2 Compression tests

Compression tests have been carried out on a more conventional Hopkinson bar setup adopting a gas gun to produce the input pulse as shown in Figure 7. The setup is about 8 m long with bars of 2.5 m and a striker bar of 0.8 m. Compression tests have been performed with a striker impact velocity of about 25 m/s.

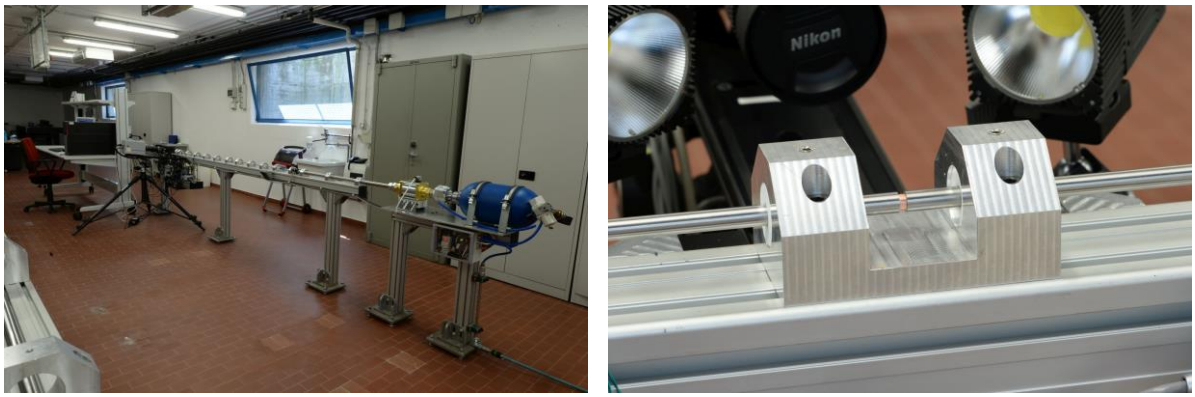

Figure 7. Testing setup for SHPB compression tests (left) and closer view of the specimen and loading equipment (right)

Table 5 summarizes the compression tests performed at the strain-rate required by the User team. In this case, because of the large size of the specimens (compared with the bar diameter and the setup loading capabilities) it has not been possible to perform tests at two strain-rate levels as performed for the tensile tests.

Table 5. High-velocity compression tests.

Test Label	Test Type	Velocity (mm/s)	Date	Material
a10	Monotonic SHPB	15000	14/07/2020	OFE Copper
a11	Monotonic SHPB	15000	14/07/2020	OFE Copper
a12	Monotonic SHPB	15000	14/07/2020	OFE Copper
a13	Monotonic SHPB	15000	14/07/2020	OFE Copper
d10	Monotonic SHPB	15000	14/07/2020	Niobium
d11	Monotonic SHPB	15000	14/07/2020	Niobium
d12	Monotonic SHPB	15000	14/07/2020	Niobium
d13	Monotonic SHPB	15000	14/07/2020	Niobium

4 Data elaboration

All recorded data in the above described tests are not directly useful to derive the force-displacement curve of the tested specimen. Some signals have to be simply scaled (because they are recorded by an AD converter in Volt) but there are some additional elaboration techniques that improve substantially the accuracy of the results derived from the acquired data. In addition, especially for the Hopkinson bar apparatus, the signal elaboration is not trivial and requires particular procedures due to the wave propagation phenomena that are exploited in this experimental technique. Sections 4.1 and 4.2 explain the principles of the data elaboration adopted to derive the force-displacement curves of each specimen in MTS and Hopkinson bar tests respectively.

In addition to conventional measurements (derived by classical mechanical transducers as for example load cells, displacement sensors, etc.), in this test campaign an intensive use of Digital Image Correlation techniques have been carried out. Since the final elaboration of photo-sequences is under responsibility of the User team, a series of preliminary validation procedures have been performed by ELSA staff to ensure high quality results. In this context, the optimal speckle size has been determined for each test to guarantee a satisfactory resolution for DIC algorithms.

4.1 MTS Servo-hydraulic testing machine

For what concerns the experimental data obtained in a test performed with a standard testing machine, the raw data are already converted in mechanical units (Forces [kN] and displacement [mm]). In any case, if it is not possible to apply an extensometer, it is better to compensate the elastic deformation of the frame structure of the testing machine (knowing the machine stiffness) to achieve a greater accuracy in the evaluation of the Young modulus of the specimen. The elaboration block diagram for this kind of test can be summarized as in Figure 8.

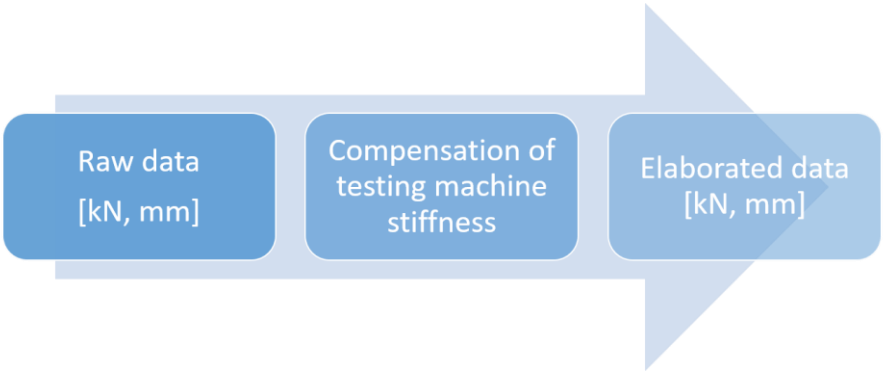

Figure 8. Elaboration block diagram for static tests

Regarding the elaboration of data from low strain-rate tests, since the machine was the same as for static tests, the adoption of the external acquisition board requires an additional step in the elaboration process. In fact, the recorded sensor signals have first to be converted in mechanical units and then elaborated, as reported in the block diagram of Figure 9. In addition, in this case, it is possible to compare the converted raw data with those recorded by the digital control unit of the testing machine (which are recorded at a lower sample rate) to ensure data consistency.

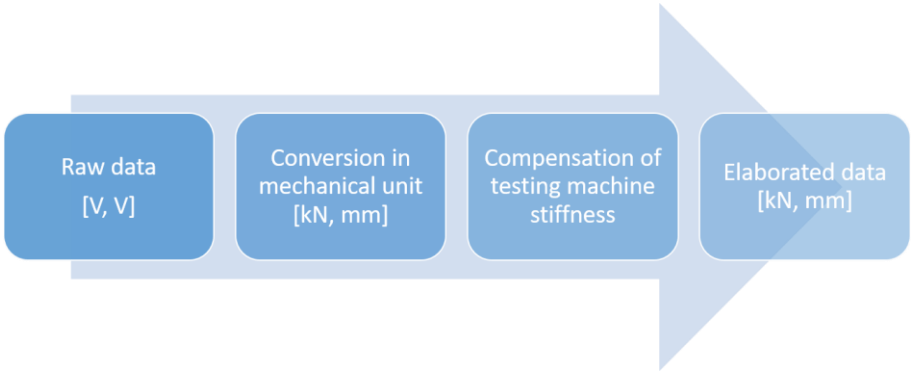

Figure 9. Elaboration block diagram for low strain-rate tests

4.2 Split Hopkinson Pressure Bar

The elaboration of data recorded in a Hopkinson bar test is substantially different from the techniques adopted in standard mechanical testing methods. Since this machine exploits the propagation of elastic waves in elastic rods, the elaboration procedure requires some typical algorithms of signal processing like Fast Fourier transforming, deconvolution, phase shifting, etc. Figure 10 presents the elaboration block diagram of the recorded signals in a Hopkinson bar test.

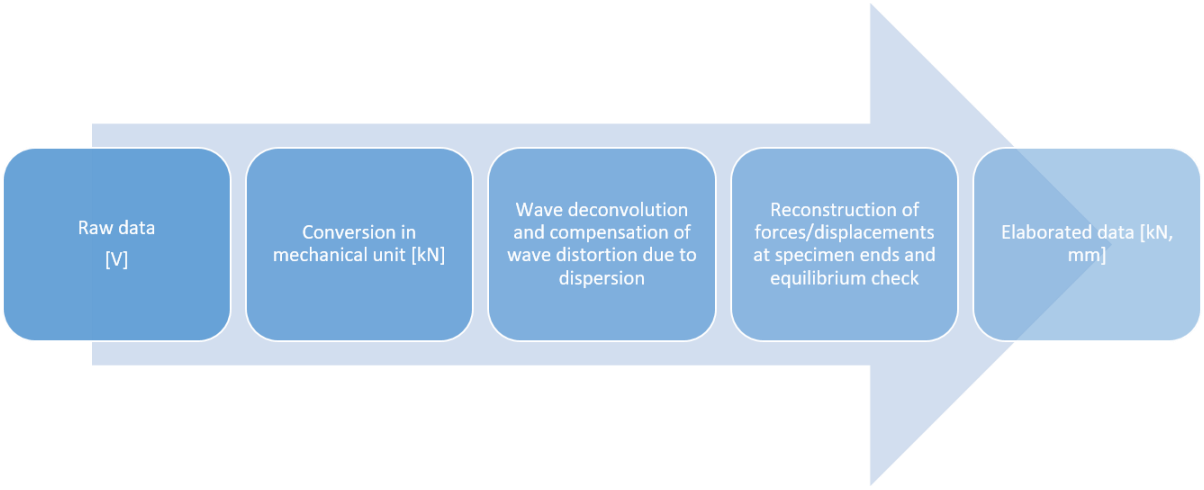

Figure 10. Elaboration block diagram for Hopkinson bar tests

Specifically, the signals, which are proportional to the input/output bar strains (recorded in three locations for each bar), are converted into forces and then with a deconvolution algorithm the two travelling waves (ascending and descending) in each bar are distinguished and the incident, reflected and transmitted waves are determined. This algorithm has to compensate for distortions due to dispersion phenomena because a wave pulse, when propagating through an elastic confined medium, changes its shape (the different frequency wave components propagate with slightly different velocities).

Knowing the ascending and descending waves in each bar, the forces and displacements at the specimen ends can be accurately reconstructed and then the equilibrium of the specimen checked. If the specimen is in equilibrium, as checked to be the case in these tests, the forces and displacements reconstructed are appropriate for the evaluation of the stress-strain curve of the tested material.

5 Database structure and data results

For the tests of the DWAM project a considerable amount of data has been stored and managed. This section provides a basic description of the database structure of the user data (raw and elaborated), which is similar to the database adopted since 2000 in the ELSA laboratory. Diagrammatically the database is organized as depicted in Figure 11.

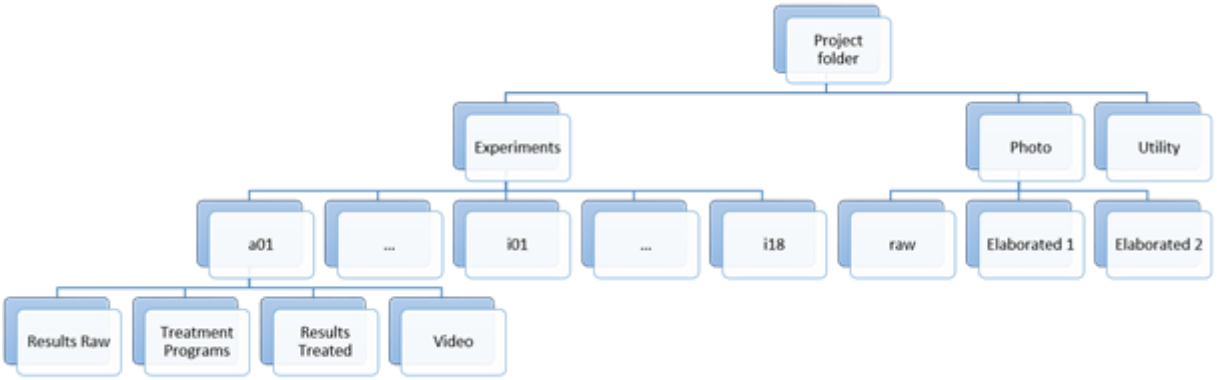

Figure 11. Database structure

The main project folder contains one excel file (*specimen.xlsx*), which contains the table with all experiments performed (test label, test type and other details about the test configurations). The main folder contains in addition:

- The *Experiments* folder. This folder contains several subfolders named with the test labels described in the *specimen.xlsx* file. In each experiment folder, there are four subfolders that contain: the raw data acquired during the experiments (*Results Raw*), the MATLAB® routines used to elaborate the data and save them in the format required by the users (*Treatment Programs*), the treated results (*Results Treated*) and the photo sequence acquired during the tests (*Video*).
- The *Photo* folder contains all the photos shot during the tests campaign. The original photos are stored in the *raw* folders while the elaborated ones (in general subsampled at 300 dpi) are saved in the *elaborated* folders (with a label that identifies the test campaign phase).
- The *Utility* folder contains some applications useful for the elaboration of the data results. In this case, this folder contains two software applications useful to open the test photo sequences.

In the next paragraphs, a small description of the data in the *Experiments* folders will be given to help the users in the elaboration phases of all experimental data.

Raw results consist of several ASCII files with the time histories of the strain-gage measurements from the points along the bars. Each file has two columns: time (s) and strain-gage signal (V). The conversion factors of each strain sensor can be found in the MATLAB® elaboration files of each test.

The elaborated data are reported in text files with four columns and headers: net specimen displacement (mm), force (kN), specimen strain and specimen stress (MPa). The elaborated data do not have a constant duration but depend on the specimen failure time. However, the time is always synchronized with the image acquisition.

6 Results overview

This section presents an overview of the main results obtained in the DWAM test campaign mainly for what concerns the force-displacement curves of tested specimens. The transformation into stress-strain curves is not trivial and requires in-depth analysis due to the specimen geometries adopted and for this reason will be presented in further scientific papers. Data will be grouped by specimen geometry. All the considerations drawn in this section do not take into account the presence of the welding in the specimen (that obviously alters the material microstructure) and consider a uniform strain field. This can be justified by the high quality of the welding technology that should not affect dramatically the material behaviour.

The DIC elaborations presented here are purely indicative of the results that could be achieved by the User team applying state-of-the-art DIC algorithms to the available photo-sequences. Obviously, DIC is essential to accurately investigate the strain field in a test campaign like this one, because of the presence of heterogeneities into the specimen.

6.1 Tensile tests ('standard' geometry)

Figure 12 presents the main results, using standard measurement techniques, in terms of force-displacement curves at different velocity/strain-rate for both tested materials. For each different velocity level, both repetitions are presented (solid and dashed lines). OFE copper presents a limited strain-rate sensitivity for what concerns yield stress, and ultimate stress. The different curves could be adequately modelled with a simple multiplicative model as normally proposed for Face-Centred Cubic (FCC) metals (for example Johnson-Cook model [3]).

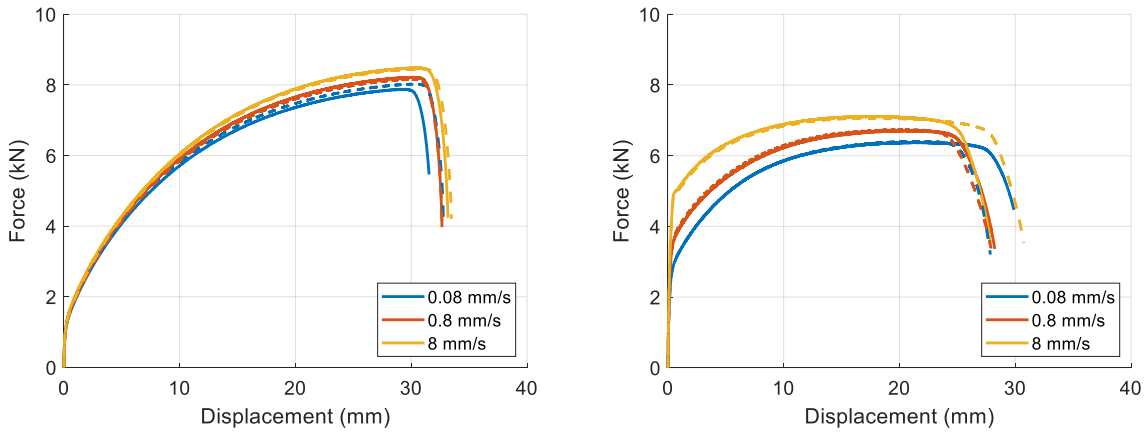

Figure 12. Tensile stress-strain curves (specimens with 'standard' geometry) for OFE copper (left) and niobium (right)

On the other hand, niobium presents a greater strain-rate sensitivity on the yield stress, and ultimate stress, which is not negligible also in the limited velocity range tested with this specimen geometry. As typically observed in Body-Centred Cubic (BCC) metals, the yield stress increases with a power law formulation and strain-hardening and strain-at-ultimate-stress decrease for increasing strain-rates. These curves could be better fitted with more complex additive/multiplicative models (for example Zerilli-Armstrong model [4]).

Moreover, for both materials, the scattering of the strain-to-failure of different tests makes it impossible to observe any well-defined trend.

Figure 13 presents a photo sequence acquired during the test on this specimen geometry (left) and a simple DIC elaboration of the sequence (right).

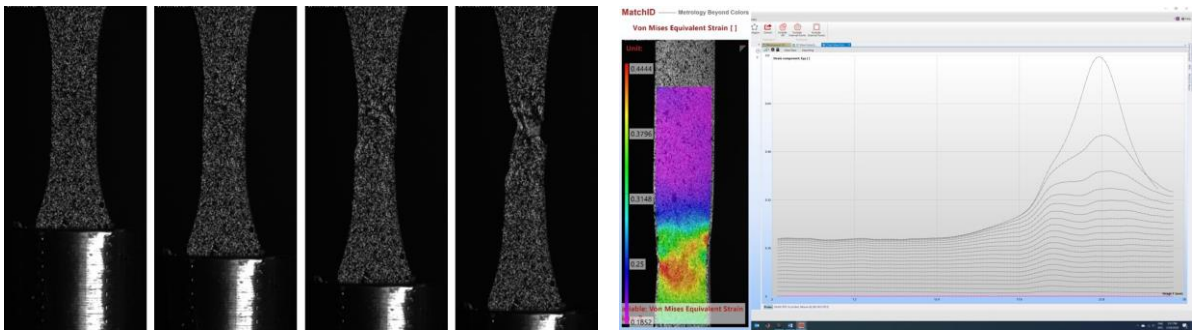

Figure 13. Example of acquired photo sequence in test f01 (left) and evolving strain map and axial strain profile from MatchID (right)

With DIC it is possible to have access to a huge amount of data monitoring the full-field strain evolution on the specimen surface. For example, it is possible to have the strain map for each test frame or the profile of the axial strain along the specimen to study the strain homogeneity during the test. As reported in Figure 13 (right), the strain increased homogeneously along the specimen's gage-length since necking occurred (lines from the bottom to the top for increasing test time). After necking, strain was concentred in this zone as clearly visible in the upper curves. No significant perturbations due to the weld have been observed in these tests.

In addition, DIC measurement helps to increase the accuracy of strain measurements derived by machine stroke, by compensating the errors induced by the equipment deformability or the specimen fixture deformation.

6.2 Tensile tests ('high strain-rate' geometry)

Figure 14 presents all the data obtained at different strain-rates for both materials on the smaller specimen geometry. The investigated velocity range passes from two orders of magnitude for the previous specimen geometry (0.08 to 8 mm/s) to six (0.01 to about 10000 mm/s). In this scenario, the influence of the strain-rate on the mechanical behaviour can be better evaluated.

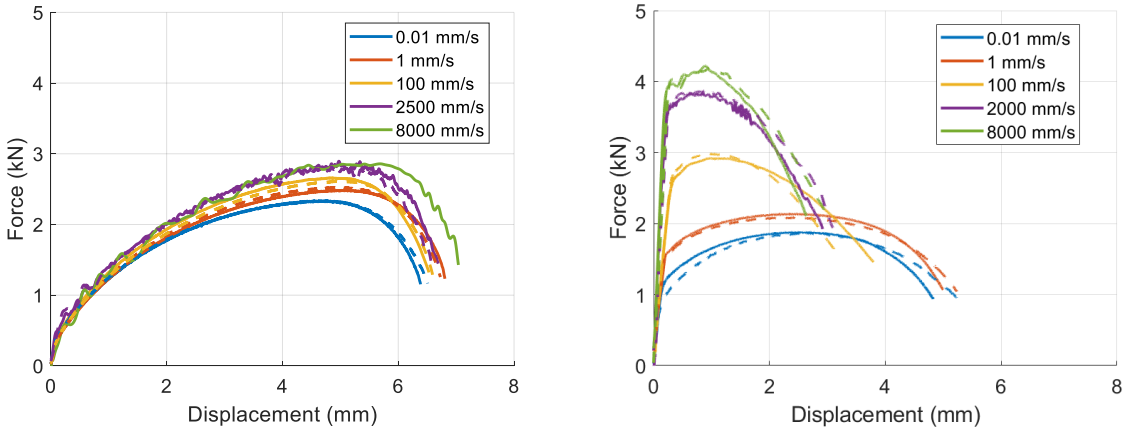

Figure 14. Tensile stress-strain curves ('high strain-rate' geometry) for OFE copper (left) and niobium (right)

As for the 'standard' geometry, OFE copper seems slightly influenced by strain-rate in terms of yield stress and ultimate stress. Also in this extended range of strain rate, data can be reasonably fitted with a simple multiplicative model (Johnson-Cook model) neglecting the increase of the strain-at-maximum-stress (for multiplicative models this parameter is strain-rate independent).

On the other hand, the niobium behaviour is confirmed to be largely influenced by strain-rate for what concerns yield stress, strain-at-maximum-stress and strain-to-failure. In addition, strain hardening seems to decrease when increasing the strain-rate. All these physical phenomena could be properly captured with the Zerilli-Armstrong model mentioned before.

Analysing a larger strain-rate interval, compared with the test on 'standard' geometry strain-to-failure of both materials exhibit well observable trends, since the data scattering remains not negligible. For copper, increasing the strain-rate, the strain-to-failure seems to slightly increase. On the contrary, the niobium strain-to-failure substantially decrease increasing the strain-rate.

Figure 15 shows on the left a photo-sequence obtained during test e02 on a niobium specimen and on the right a simple elaboration using the DIC approach. Especially for niobium, the strain field of the specimen gage-section seems less uniform compared to tests on larger specimens. It is possible to observe two peaks in the strain field along the specimen's gage-length that underline different mechanical properties between the base material and the one in the fusion zone of the welding. This discontinuity becomes more evident as the strain increases (lines from the bottom to the top) but it is still present before necking.

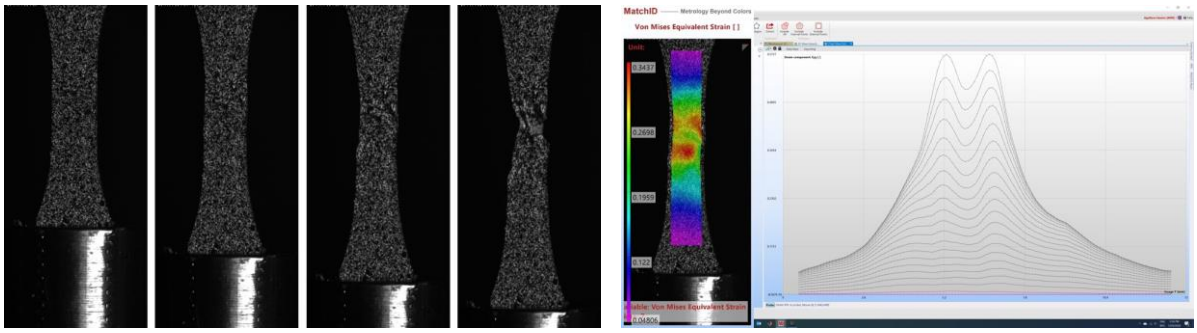

Figure 15. Example of acquired photo sequence in e02 test (left) and evolving strain map and axial strain profile (right)

6.3 Compression tests

Figure 16 presents the force-displacement curves obtained by compression tests at different velocities. The investigated velocity range covers more than six orders of magnitude (between 0.004 to about 15000 mm/s) and makes possible to draw accurate conclusions about the material strain-rate sensitivity.

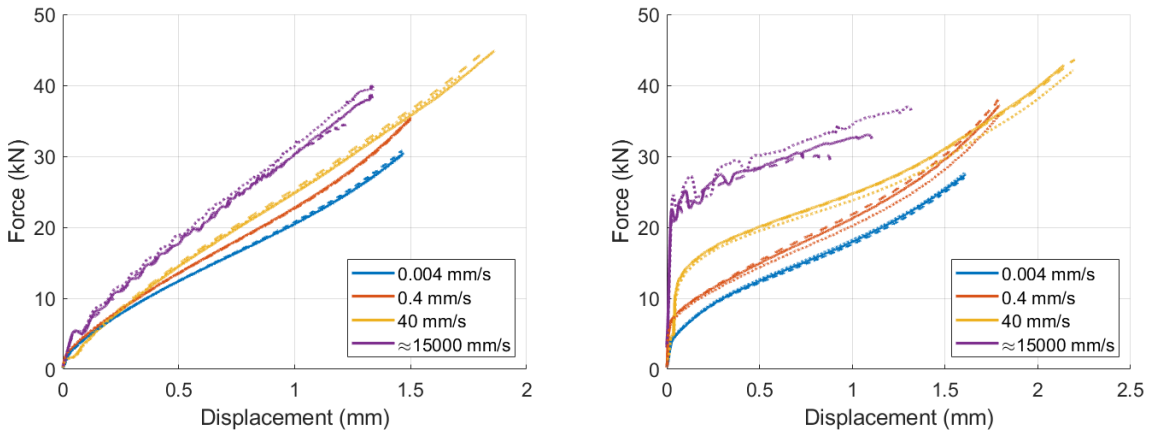

Figure 16. Compression stress-strain curves for OFE copper (left) and niobium (right)

The mechanical behaviour of both materials observed in tensile tests is confirmed by compression ones where, due to the ductility of the investigated materials, no specimen failed. Niobium confirms a larger strain-rate sensitivity compared with OFE copper with the differences already discussed for tensile tests.

DIC remains useful to observe the irregularity in the strain field of the specimens. However, the application of this methodology is more complex for compression tests, due to the cylindrical specimen geometry, and it is not investigated in this report.

Figure 17 shows the photo sequence concerning the experiment d01 on a niobium specimen. The non-symmetrical barrel shape of the specimen in the last images have to be further investigated. This phenomenon seems too accentuated to be caused by small differences in the friction coefficients between

the specimen and the rig plates and no particular anisotropic structures have been experimentally observed (in terms of grain size and distribution between the top and the bottom specimen ends).

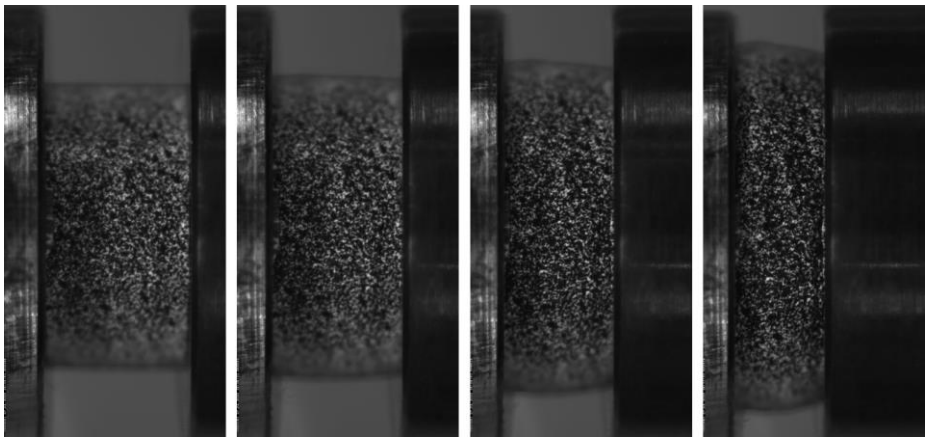

Figure 17. Example of acquired photo sequence in d01 test

7 Conclusions

This report has presented the main technical aspects of the DWAM test campaign carried out in the context of the JRC OPEN ACCESS activity at the HopLab laboratory. A description of the test machines and elaboration procedures has been reported to help the user effectively use the data results. The large amount of data, in terms of sensor signal histories and image acquisitions, has been organized following the established structure of the ELSA laboratory database, and stored on the JRC BOX for a fast data exchange with the potential users.

The project has reached its objectives and the activity is deemed to be a success by both parties. The experimental data obtained are considered to be of high quality and of significant scientific interest for the advanced manufacturing processes and materials investigated, and they could constitute a solid starting point for future collaborative research.

References

[1] ASTM International, "ASTM B170-99(2015), Standard Specification for Oxygen-Free Electrolytic Copper—Refinery Shapes," West Conshohocken, PA, 2015. doi: 10.1520/B0170-99R15.

[2] International Organization for Standardization, "ISO 4136:2012 - Destructive tests on welds in metallic materials - Transverse tensile test." 2012, [Online]. Available: https://www.iso.org/standard/62317.html.

[3] Johnson, G. R., and W. H. Cook, "Fracture Characteristics of Three Metals Subjected to Various Strains, Strain rates, Temperatures and Pressures," Engineering Fracture Mechanics, vol. 21, no. 1, pp. 31–48, 1985.

[4] Zerilli, Frank J., & Armstrong, Ronald W. (1987). Dislocation-mechanics-based constitutive relations for material dynamics calculations. http://doi.org/10.1063/1.338024.

List of figures

List of tables

GETTING IN TOUCH WITH THE EU

In person

All over the European Union there are hundreds of Europe Direct centres. You can find the address of the centre nearest you online (european-union.europa.eu/contact-eu/meet-us_en).

On the phone or in writing

Europe Direct is a service that answers your questions about the European Union. You can contact this service:

— by freephone: 00 800 6 7 8 9 10 11 (certain operators may charge for these calls),

— at the following standard number: +32 22999696,

— via the following form: european-union.europa.eu/contact-eu/write-us_en.

FINDING INFORMATION ABOUT THE EU

Online

Information about the European Union in all the official languages of the EU is available on the Europa website (european-union.europa.eu).

EU publications

You can view or order EU publications at op.europa.eu/en/publications. Multiple copies of free publications can be obtained by contacting Europe Direct or your local documentation centre (european-union.europa.eu/contact-eu/meet-us_en).

EU law and related documents

For access to legal information from the EU, including all EU law since 1951 in all the official language versions, go to EUR-Lex (eur-lex.europa.eu).

Open data from the EU

The portal data.europa.eu provides access to open datasets from the EU institutions, bodies and agencies. These can be downloaded and reused for free, for both commercial and non-commercial purposes. The portal also provides access to a wealth of datasets from European countries.

The European Commission's science and knowledge service

Joint Research Centre

JRC Mission

As the science and knowledge service of the European Commission, the Joint Research Centre's mission is to support EU policies with independent evidence throughout the whole policy cycle.

EU Science Hub
joint-research-centre.ec.europa.eu

 @EU_ScienceHub

 EU Science Hub - Joint Research Centre

 EU Science, Research and Innovation

 EU Science Hub

 EU Science

Publications Office
of the European Union